8.2 RADIATIVE IMPACTS OF ABSORBING AEROSOLS ON TROPICAL MARITIME BOUNDARY LAYER AND TRADE WIND CUMILI

Hailong Wang[1], Greg M. McFarquhar[1] and Wojciech Grabowski[2]

[1]University of Illinois, Dept. of Atmospheric Sciences, Urbana, IL
[2]National Center for Atmospheric Research (NCAR), Boulder, CO

1. INTRODUCTION

This study presents three-dimensional cloud resolving model (CRM) simulations of aerosol effects on boundary layer and trade wind cumuli over the Indian Ocean region. Trade wind cumuli are ubiquitous over much of the tropical oceans. Although the importance of trade cumuli to weather and climate has long been recognized (e.g., Riehl et al. 1951; Tiedtke et al. 1988), our understanding of their role in global water and energy cycles and their treatment in climate models is very poor. Anthropogenic aerosols emitted into the atmosphere alter the Earth's radiative forcing and climate both through their direct radiative effect and indirect effects of increasing cloud albedo (Twomey 1974, 1977) and lifetime (Albrecht 1989). Aerosols containing black carbon (soot) may also alter cloud cover and liquid water content through the absorption of solar radiation. This is known as the semi-direct effect (Hansen et al. 1997).

The Indian Ocean Experiment (INDOEX) was a major field study aimed at understanding the regional and global climate forcing associated with the anthropogenic haze that spread over the tropical northern Indian Ocean during the winter monsoon. Extensive observations during INDOEX (Ramanathan et al. 2001) show that trade wind cumuli with a low fractional coverage were embedded in the widespread haze. Heymsfield and McFarquhar (2001) reported the observed evidence of aerosol effects on cloud properties. Using a large eddy simulation model, Ackerman et al. (2000) found a decrease of trade wind cumulus cloud cover and liquid water path when solar heating from soot was taken into account.

There is considerable uncertainty in estimates of indirect and semi-direct effects, which severely limits the ability to represent these processes in large-scale models needed to predict the global forcing associated with such processes. To date, no satisfactory estimates of global-annual-mean aerosol forcing due to semi-direct or indirect effects have been achieved, which is partly caused by the coarse resolution and the uncertainties regarding the treatment of clouds and aerosols in the large-scale models. As argued by Grabowski (2000), quantitative estimates of aerosol effects on cloud microphysics may best be studied within the context of CRM because of complicated interactions among cloud dynamics, cloud microphysics, radiative processes and surface processes. The purpose of this study is to better characterize the nature and magnitude of semi-direct and indirect regional effects by conducting three-dimensional CRM simulations on diurnal cycles of trade wind cumuli in the Indian Ocean region, where processes such as the effect of soot absorption can be represented in finer detail than possible in large-scale models. The premise of the modeling simulations can be tested against observations of these quantities obtained during INDOEX, which come from a combination of in-situ and remote sensing observations (e.g., McFarquhar et al., 2004).

Corresponding author address: Hailong Wang, University of Illinois, Dept. of Atmospheric Sciences, 105 S. Gregory Street, Urbana, IL, 61801-3070, Email: hailong@atmos.uiuc.edu.

2. CLOUD RESOLVING MODEL SIMULATIONS

2.1 Model Description

The CRM used for this study is the Eulerian version of the non-hydrostatic Eulerian/semi-Lagrangian (EULAG) anelastic fluid model described by Smolarkiewicz and Margolin (1997). It uses a forward-in-time approach for all prognostic fields. The sub-grid turbulent processes are parameterized using the TKE approach of Schumann (1991). The model includes the moist precipitation thermodynamics of Grabowski and Smolarkiewicz (1996). The Kessler-type warm rain parameterization of small-scale thermodynamics (Kessler 1969) or autoconversion of cloud water into rainwater (Berry 1967, 1968) is used in the model. Cloud droplet number concentration (CDNC) is prescribed and different values would be used for clean or polluted environment. The effective radius of cloud droplet is calculated interactively using the scheme and parameters proposed by McFarquhar and Heymsfield (2001). The δ-four-stream radiative transfer model (Liou et al. 1988; Fu and Liou 1992) interactively computes the broadband solar and infrared radiative properties of clouds, aerosol including soot, nongray gases and air molecules.

The lateral boundary conditions in EULAG model are doubly periodic. The model bottom is flat and free-slip. In order to minimize the gravity wave energy accumulation at the upper lid, and reflection from it, damping absorbers are employed in the vicinity of the model top boundary. The model takes initial sounding and sea surface temperature (SST) as inputs. Surface heat flux and moisture flux are thereby computed using the simplified Fairall et al.'s (1996) bulk formulae.

2.2 Experimental Setup

Simulations with time step increment of 2.5s are performed in a numerical domain of 64X64X75 grid mesh with a uniform grid spacing of 100m in the

horizontal and 40m in the vertical. A temperature and water vapor mixing ratio pseudo-random perturbation of 0.2°C and 0.2 g kg^{-1} are applied in the mixed layer to initialize convection. Simulations on diurnal evolution with varying external forcing are run for 30 hours starting from local midnight. To save computational time but maintain sufficient accuracy, radiative forcing is updated every 2.5 minutes in the model.

Table 1 Characteristics of the numerical simulations

Run	Aerosol			CDNC (cm^{-3})
	Type	Soot Location*	$\tau_{0.55\mu m}$	
CONC	Background	-	0.18	50
CONP	Background	-	0.18	350
NOSUN	Background	-	0.18	50
SOOTT	With Soot	Throughout B.L.	0.33	350
SOOTA	With Soot	Above Cloud Layer	0.23	350
SOOTB	With Soot	Below Cloud Layer	0.22	350
SOOTC	With Soot	Within Cloud Layer	0.22	350

Note: Wherever no soot exists, there exists the background aerosol.

Table 1 summarizes the characteristics of the numerical simulations designed for diurnal evolution of trade cumuli. The single scattering albedo and extinction coefficient of the absorbing aerosols (background aerosols) at 0.55μm are computed as 0.889 (0.996) and 0.124 (0.06) respectively. For these idealized vertical distributions, aerosols are homogeneously distributed in the layers. The first two control runs are designed to investigate the indirect effect of aerosols. The only difference between CONC and CONP is the CDNC, which is prescribed in bulk cloud microphysics. CDNC of 50cm^{-3} and 350cm^{-3} close to median value for clean and polluted cloud respectively reported by Heymsfield and McFarquhar (2001). For comparison, the NOSUN run is identical to CONC, except that solar radiation is taken away. Four other experiments with soot at different location as indicated in table 1 are preformed to study the effects of strong absorbing aerosols and its vertical distribution on cloud formation and development.

3. CASE DESCRIPTION AND MODEL INITIATION

During INDOEX, there were 5 gradient flights when the NCAR C-130 made long low-level transits in and below cloud flying south from Male (4˚11'N, 73˚32'E) to approximately 7˚S in order to depict the meridional variation of cloud properties. On the return leg to Male, the C-130 flew through the middle troposphere collecting solar and infrared radiometer data, and released dropsondes to sample the thermodynamic structure of the atmosphere at fine resolution. This provides the environmental profiles needed to initiate the CRM simulations. Initial vertical profiles in this study are obtained by merging 13 dropsondes within a temporal range of 3 hours in March 4, 1999 during INDOEX, as shown in Figure 1. A well-mixed layer exists below 600m. Above this layer, a conditionally unstable layer extends all the way up to the top of model atmosphere. Being different from initial temperature profile used by Ackerman et al. (2000), there is no inversion cap over the top of boundary layer, which allows the vertical development of trade wind cumuli. A weak southeasterly wind is blowing over the model atmosphere. SST for March 4 estimated using retrievals from the Tropical Rainfall Measuring Mission (TRMM) Microwave Imager (TMI) is 29.2°C. No diurnal variation is imposed because Webster et al. (2002) measured diurnal variations in SST over the Indian Ocean of only about 0.5°C.

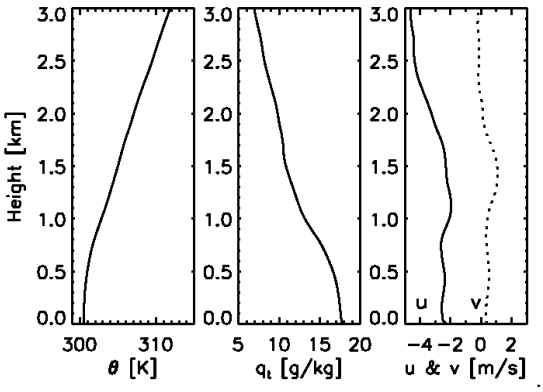

Figure 1. The vertical profiles of potential temperature (θ), total water mixing ratio (q_t) and horizontal wind speeds (u, v) from merging dropsondes in Mar. 4 1999.

4. SIMULATION RESULTS

The study evaluates the indirect and semi-direct effects of aerosol on trade wind cumuli as well as on the marine boundary layer. Figure 2 depicts a 3-D representation of simulated instantaneous cloud fields from CONP. The effect of solar heating on cloud properties is seen through the reduction in cloud cover in the afternoon. Following the cloud classification of fair-weather cumulus by Stull (1985), simulated trade wind cumuli can be classified into three categories: forced, active and passive clouds. Forced clouds form in the tops of mixed layer (ML) thermals, and the cloud top

never reaches its level of free convection (LFC). Active clouds, which are also triggered by ML thermals, can reach LFC and become positively buoyant. Updrafts keep moving ML air into the active cloud base and venting pollutants from the ML. Passive clouds are the decaying remnants of formerly active clouds. They no longer vent ML air and bottoms of these clouds are diffuse as cloud droplets evaporate.

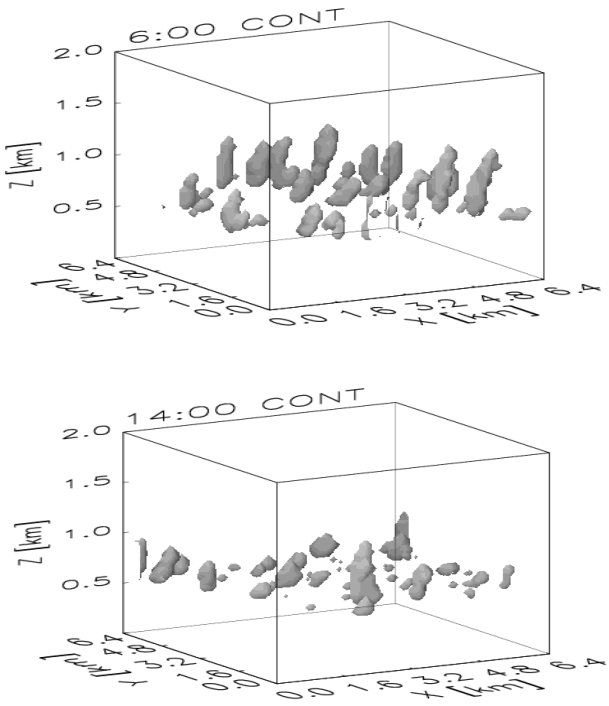

Figure 2. Snapshots of the model domain taken at 6:00 and 14:00 from control run CONP, the 0.01g/kg isosurface of cloud water mixing ratio is plotted. Note that the vertical scale is stretched relative to the horizontal.

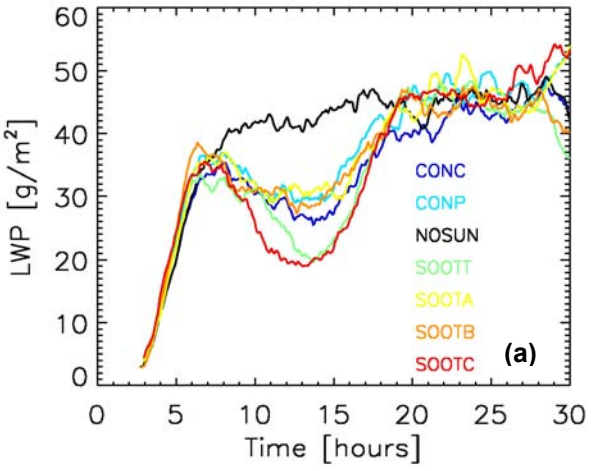

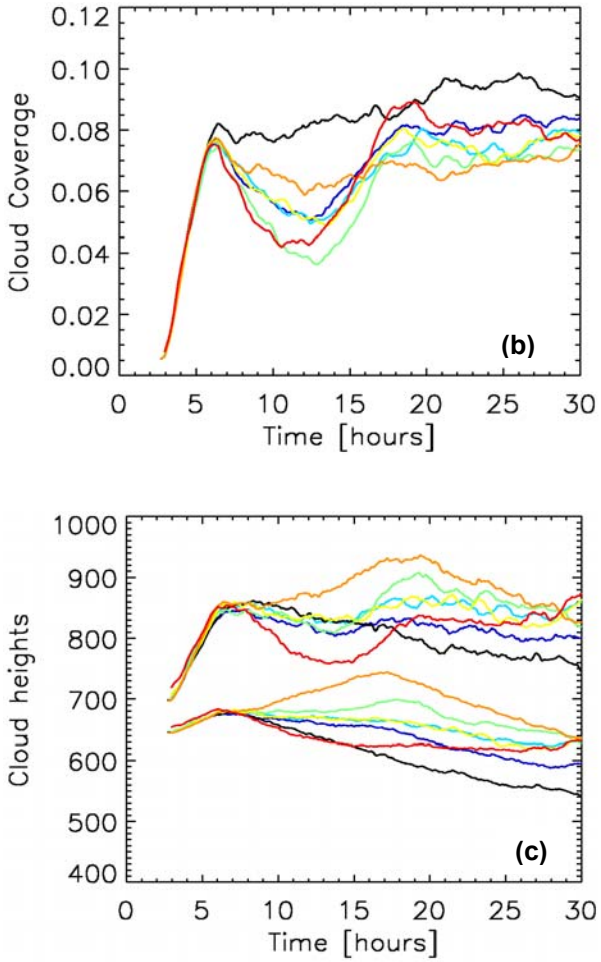

Figure 3. Simulated diurnal evolutions of **(a)** LWP averaged over cloudy grids, **(b)** cloud fraction and **(c)** average cloud top and base height. All the curves have been smoothed over 3 hours.

Figure 3 shows the simulated diurnal evolutions of LWP, cloud coverage and cloud heights, where LWP and cloud heights are taken average over all cloud grid columns. The EULAG model can simulate the significant daytime (6:00-18:00) reduction in magnitude of cloud coverage and LWP. Pronounced differences among all runs are seen indicating that these cloud properties are sensitive not only to the concentration and absorption property of aerosols, but also to their vertical distribution, as shown from simulations on marine stratocumulus by Johnson et al. (2004). The daytime-averaged LWP varies between 26.6 g m^{-2} for SOOTC to values of 28.6, 32.4 and 32.9 g m^{-2} for SOOTT, SOOTB and SOOTA, while cloud coverage varies between 5.3% for SOOTT to values of 5.8, 6.1 and 6.7% for SOOTC, SOOTA and SOOTB. The magnitudes of cloud coverage between 4 and 10% are consistent with estimates of 0.06 (0.08) for polluted (clean) environment made by multi-channel radiometer (MCR) on board C-130 aircraft during INDOEX and of 0.09 obtained by the

Multi-angle Imaging Spectoradiometer (MISR) during the winter monsoon in years between 2001 and 2003 (McFarquhar et al. 2004). Simulated LWPs also close to estimates from observations of liquid water content reported by Heymsfield and McFarquhar (2001). These agreements with observations suggest that the EULAG model can reasonably simulate the marine trade wind boundary layer and trade wind cumuli statistics. Moreover, as seen in Figure 4, cloud coverage and LWP in three extended runs show similar diurnal variations in two days, which indicates that the simulated trends are stable, not adjustments to initial conditions. Ackerman et al. (2000) simulated the effect of soot on diurnal variations of trade wind cumuli cloud coverage and LWP with a large eddy model, which also solves anelastic equations, but their simulations were initialized by soundings with strong inversion over marine boundary layer. As a result, LWP and cloud coverage of trade wind cumuli from their simulations are significantly larger than those of ours. For cloud heights, as suggested in Fig. 2, taking account of those forced clouds would largely reduce average cloud top heights. This at least partly explained why simulated average cloud top heights are much lower than observations estimated by McFarquhar et al. (2004). On the other hand, the difference in methods to obtain average cloud heights between observation and model simulation should also account for part of the discrepancy, which will be improved in future simulations.

To better understand variations in cloud properties between simulations seen in Fig. 3 and Fig. 4, vertical profiles of domain average shortwave and total heating rate are shown in Figure 5. The differences among all runs are mainly due to the concentration and vertical distribution of soot, which gives an extra 1 K day^{-1} of shortwave heating. There are also some differences in longwave cooling rate, which are not shown here. The total radiative effect in the atmosphere is cooling.

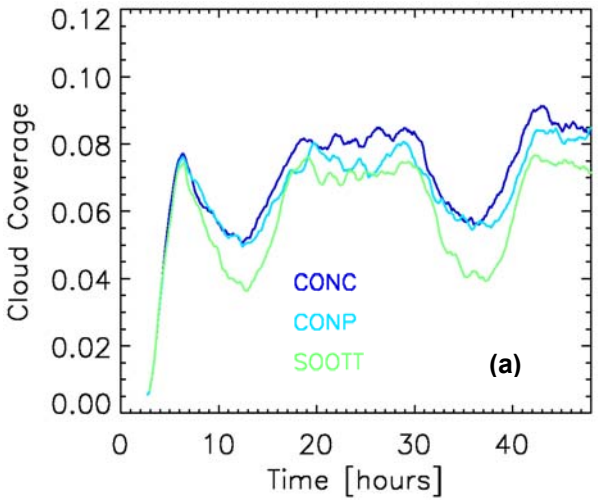

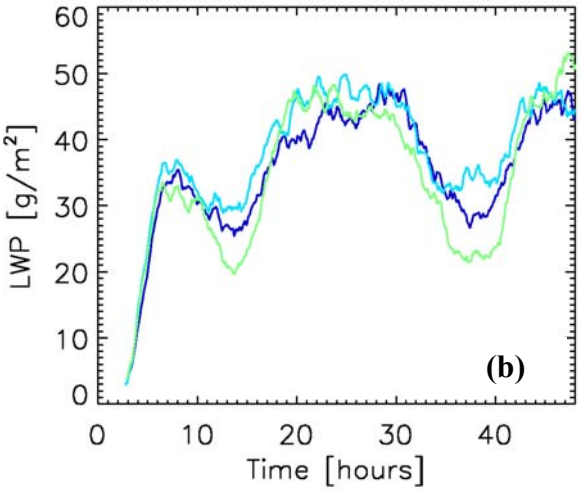

Figure 4. Simulated diurnal evolutions of **(a)** cloud coverage and **(b)** LWP that are extended to 48 hours. All the curves have been smoothed over 3 hours.

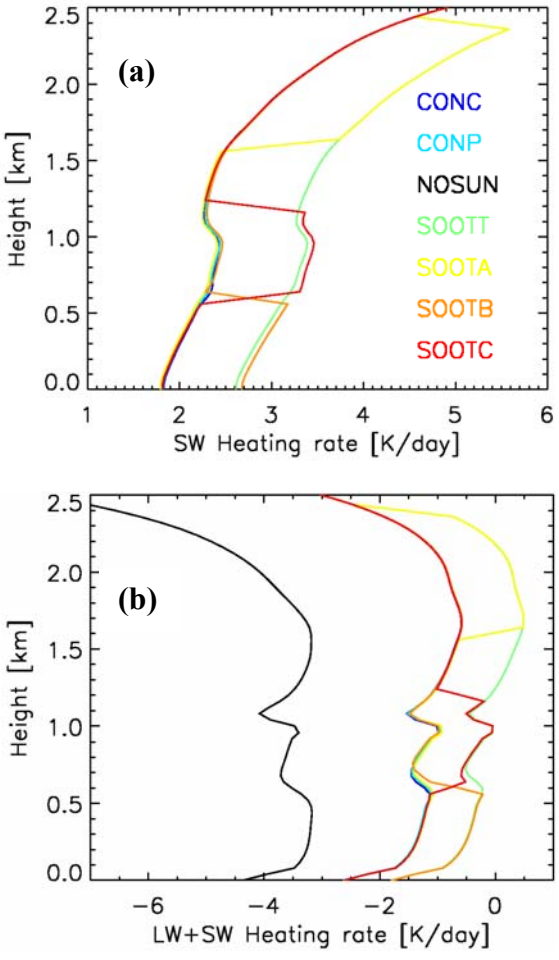

Figure 5. Model computed domain average **(a)** shortwave heating rate and **(b)** total (shortwave plus longwave) heating rate vertical profiles.

Daytime domain average vertical profiles of total water mixing ratio (q_t), potential temperature (θ), updrafts and downdrafts are plotted in Figure 6 and Figure 7. These thermodynamic variables are also sensitive to both concentration and vertical distribution of absorbing aerosols. Differences in θ of lower boundary layer are mainly caused by absorption of solar radiation. However, the differences in q_t are mostly due to the vertical advection of water, which can be explained with the governing equations, and the simulated downdrafts and updrafts are highly correlated with q_t. Low level temperature and moisture partly determine the surface fluxes of heat and moisture, which can also feedback on thermodynamic variables, then they will affect the boundary layer cloud formation and development all together.

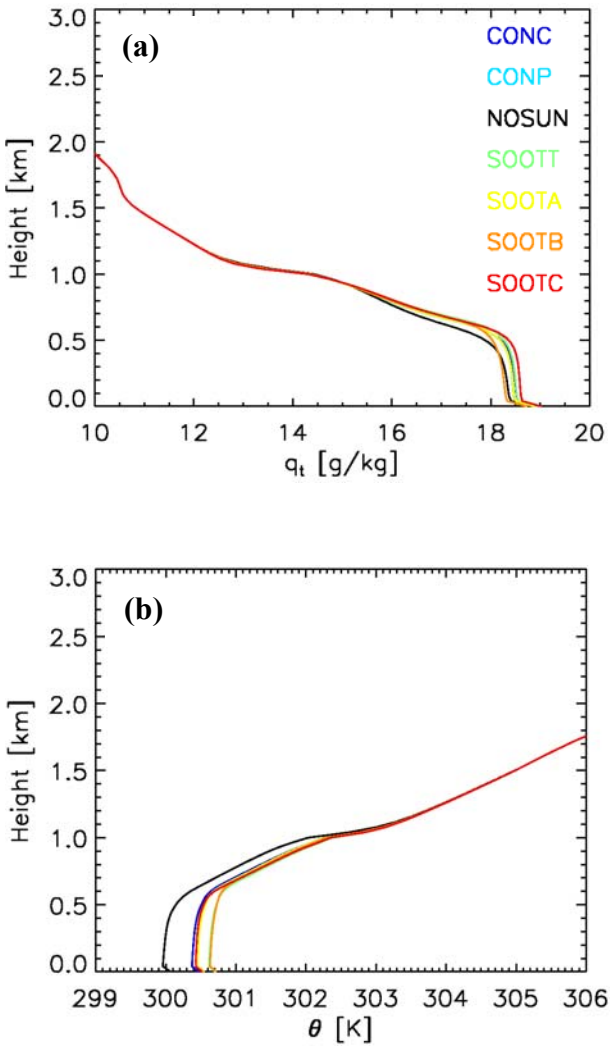

Figure 6. Daytime domain averaged vertical profiles of **(a)** total water and **(b)** potential temperature.

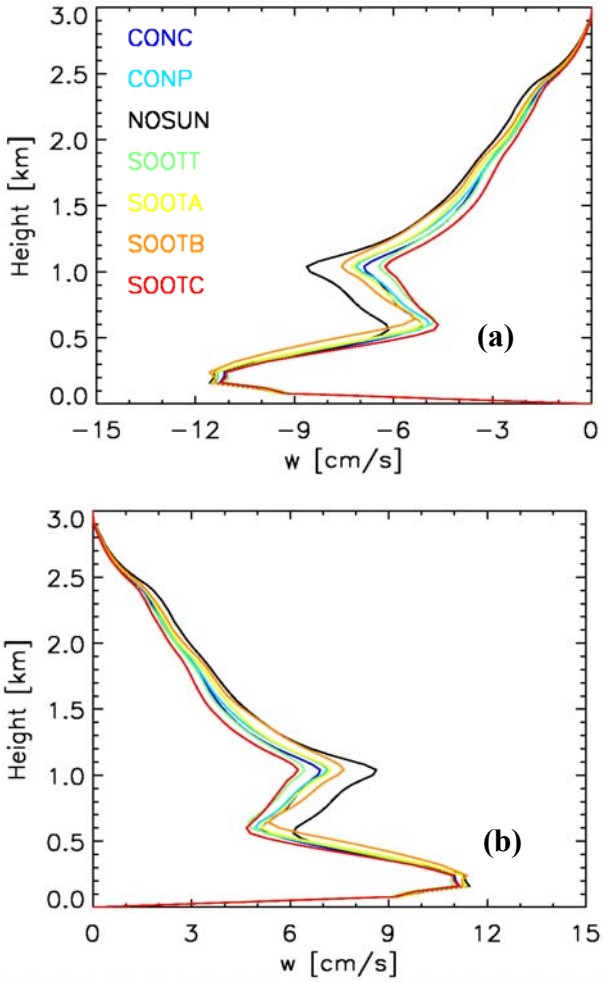

Figure 7. Daytime domain averaged vertical profiles of **(a)** downdrafts and **(b)** updrafts.

5. FORCING ESTIMATES BASED ON THE MODEL SIMULATIONS

In order to understand the significance of the differences between the simulations, estimates of semi-direct and indirect forcing are separately computed for each of the simulations extending definitions proposed by Keil and Haywood (2003). The direct forcing, f_{direct}, the difference between the clear-sky net flux observed with and without the presence of soot aerosols at either the top of the atmosphere or surface is given by

$$f_{direct} = F_{net}(soot, no\ cloud) - F_{net}(background, no\ cloud) \quad (1)$$

where F_{net} is the net flux (downwelling flux minus upwelling flux) for the appropriate simulation. The total forcing, f_{total}, is defined by

$$f_{total} = F_{net}(soot, polluted\ cloud) - F_{net}(background, clean\ cloud) \quad (2)$$

and gives the difference between the simulation including the presence of clouds with absorbing aerosols (SOOTT, SOOTA, SOOTB or SOOTC) and the simulation with the clean clouds (CONC). The combination of the direct and semi-direct forcing, $f_{semi+direct}$, is defined by

$$f_{semi+direct} = F_{net}(soot, polluted\ cloud) - F_{net}(background, polluted\ cloud) \quad (3)$$

and shows the direct effect of the soot aerosols on the radiative budget. The indirect forcing, $f_{indirect}$, shows the effect of the background aerosols on the cloud properties and is defined by

$$f_{indirect} = F_{net}(background, polluted\ cloud) - F_{net}(background, clean\ cloud) \quad (4)$$

and is hence equivalent to $f_{total} - f_{semi+direct}$. Finally, the semi-direct forcing may then be defined by

$$f_{semi} = f_{semi+direct} - f_{direct} \quad (5)$$

and shows how the absorption of aerosols are affecting cloud properties.

Table 2 summarizes the radiative forcings derived from the simulations that consider the presence of absorbing soot aerosols at different layers in the atmosphere. The direct forcing at the surface varies substantially because of the differences on the optical depth and relative location of absorbing soot. The trends in total forcing are similar to those in direct forcing because direct forcing is dominant at the surface.

Table 2 Simulated aerosol radiative forcing

W m^{-2}		SOOTT	SOOTA	SOOTB	SOOTC
f_{total}	TOA	-1.0	-1.2	-2.8	-0.5
	SRF	-15.1	-6.8	-6.7	-3.8
f_{direct}	TOA	-1.2	-0.1	-0.9	-0.5
	SRF	-14.8	-5.5	-4.6	-3.7
f_{semi}	TOA	1.5	0.3	-0.6	1.3
	SRF	1.4	0.4	-0.4	1.6
$f_{indirect}$	TOA	-1.4	-1.4	-1.4	-1.4
	SRF	-1.7	-1.7	-1.7	-1.7

The semi-direct forcing, f_{semi}, varies by up to 2.0 W m^{-2} between simulations at the surface and by up to 2.1 W m^{-2} at the top of the atmosphere. The vertical distribution of aerosols in the atmosphere can cause the surface forcing to vary from positive forcing of up to 1.6 W m^{-2} at the surface for soot confined to clouds to negative forcing of -0.4 W m^{-2} for the case that soot is exclusively below cloud. At the top of the model domain, the forcing can also vary from a positive value of 1.5 W m^{-2} for SOOTT to a negative value of -0.6 W m^{-2} for SOOTB. Hence, in the same way radiative forcing estimates for marine stratocumulus have been shown to critically depend on the vertical profile of absorbing aerosols (Johnson et al. 2004), the radiative forcing for trade wind cumuli also depends on the vertical profile of absorbing aerosols. This may suggest that closer to the sources of soot where aerosols are likely confined within mixed layers aerosols may have negative semi-direct forcing, whereas further from the sources where aerosols are likely higher there may be positive forcing. Note that for these simulations the indirect forcing is the same for all simulations because no dependence on the absorbing properties of aerosols was assumed for nucleation.

6. SUMMARY

In this study, the impact of absorbing soot on the formation and evolution of trade wind cumuli in the Indian Ocean region has been examined. The EULAG model can reasonably simulate the diurnal evolution of trade wind cumuli. Simulations show that cloud properties are sensitive not only to the concentration and absorption properties of aerosol, but also to its vertical distribution. Absorbing aerosols within clouds enhance the daytime reduction of cloud cover and LWP, but the presence of soot below cloud partially compensates the daytime reduction of cloud cover and LWP; absorbing aerosols above cloud have similar diurnal cycles as simulations without absorbing aerosols. It is revealed that the impact of absorbing aerosol on vertical velocities plays a critical role in affecting the boundary layer humidity profile and cloud properties.

The magnitudes of the simulated cloud fraction and liquid water contend are very close to observations obtained during INDOEX. The simulated indirect and semi-direct effects have an important impact on cloud properties, and therefore, on the water and energy budgets of the simulated region. A future study with a bin-resolving microphysics will provide better representations of cloud condensation and drizzle formation so that an improved estimate of the indirect effect can be derived.

7. ACKNOWLEDGEMENTS

The National Aeronautics and Space Administration Global Water and Energy Cycle (GWEC) Research and Analysis Program supported this research. The findings of this research do not necessarily represent the views of the agency. The dropsonde data were obtained from NCAR's Joint Office of Science Support (JOSS); A. Heymsfield was the PI for these data during INDOEX. TMI data are produced by Remote Sensing Systems and sponsored by NASA's Earth Science Information Partnerships (ESIP) and by NASA's TRMM science team.

8. REFERENCES

Ackerman, A.S., O.B. Toon, D.E. Stevens, A.J. Heymsfield, V. Ramanathan, and E.J. Welton, 2000: Reduction of tropical cloudiness by soot. *Science*, **288**, 1042-1047.

Albrecht, B.A., 1989: Aerosols, cloud microphysics, and fractional cloudiness. *Science*, **245**, 1227-1230.

Berry, E.X., 1967: Cloud droplet growth by collection, *J. Atmos. Sci.*, *24*, 688-701.

Berry, E.X., 1968: Modification of the warm rain process. In: Proceedings of the first national conference on weather modification, Albany, NY, April 28-May 1, American Meteorological Soc., pp.81-88.

Fairall, C.W., E.F. Bradley, D.P. Rogers, J.B. Edson, and G.S. Young, 1996: Bulk parameterization of air-sea fluxes for Tropical Ocean-Global Atmosphere Coupled-Ocean Atmosphere Response Experiment. *J. Geophys. Res*., **101**, 3747-3764.

Fu, Q., and K.N. Liou, 1992: On the correlated k-distribution method for radiative transfer in nonhomogeneous atmospheres. *J. Atmos. Sci.*, **49**, 2139-2156.

Grabowski, W.W., 1999: A parameterization of cloud microphysics for long-term cloud-resolving modeling of tropical convection. *Atmos. Res.*, **52**, 17-41.

Grabowski, W.W., 2000: Cloud Microphysics and the Tropical Climate: Cloud-Resolving Model Perspective. *J. Climate*, **13**, 2306–2322.

Grabowski, W.W., and P.K. Smolarkiewicz, 1996: On two-time level semi-Lagrangian modeling of precipitating clouds. *Mon. Wea. Rev.*, **124**, 487-497.

Hansen, J., M. Sato, and R. Ruedy, 1997: Radiative forcing and climate response*, J. Geophys. Res., **102***, 6831-6864.

Heymsfield, A.J., and G.M. McFarquhar, 2001: Microphysics of INDOEX clean and polluted trade cumulus clouds. *J. Geophys. Res.*, **106**, 28653-28674.

Johnson, B.T., K.P. Shine, and P.M. Forster, 2004: The semi-direct aerosol effect: Impact of absorbing aerosols on marine stratocumulus, *Quart. J. Roy. Metero. Soc.*, **130**, 1407-1422.

Keil, A., and J. M. Haywood (2003): Solar radiative forcing by biomass burning aerosol particles during SAFARI 2000: A case study based on measured aerosol and cloud properties, *J. Geophys. Res.*, *108*(D13), 8467, doi:10.1029/2002JD002315

Kessler, E., 1969: On the distribution and continuity of water substance in atmospheric circulations. Meteor. Monogr., No. **32**, *Amer. Meteor. Soc.*, 84 pp.

Liou, K.N., Q. Fu, and P.T. Ackerman, 1988: A simple formulation of the delta-four-stream approximation for radiative transfer parameterizations. *J. Atmos. Sci.*, **45**,1940-1948.

McFarquhar, G.M., and A.J. Heymsfield, 2001: Parameterizations of INDOEX microphysical measurements and calculations of cloud susceptibility: applications for climate studies. *J. Geophys. Res.*, **106**, 28 675-28 698.

McFarquhar, G.M., S. Platnick, L. Di Girolamo, H. Wang, G. Wind, and G. Zhao, 2004: Trade Wind Cumuli Statistics in Clean and Polluted Air over the Indian Ocean from In-situ and Remote Sensing Measurements, *Geophys. Res. Lett.*, in press.

Ramanathan, V., and 39 Co-authors, 2001: Indian Ocean Experiment: An integrated analysis of climate forcing and effects of the great Indo-Asian haze. *J. Geophys. Res.*, **106**, 28371-28398.

Riehl, H., C. Yeh, J. S. Malkus, and N. E. LaSeur, 1951: The north-east trade of the Pacific Ocean. *Quart. J. Roy. Meteor. Soc.,* **77**, 598–626.

Schumann, U., 1991:Subgrid length-scales for large-eddy simulations of stratisfied turbulence. *Theor. Comput. Fluid Dyn.*, **2**, 279-290.

Smolarkiewicz, P.K., and L.G. Margolin, 1997: On forward-in-time differencing in fluids: An Eulerian/semi-Lagrangian nonhydrostatic model for stratified flows. *Atmosphere-Ocean Special*, **35**, 127-152.

Tiedtke, M., Heckley, W. A., and J. Slingo, 1988: Tropical forecasting at ECMWF: The influence of physical parmetrization on the mean structure of forecasts and analyses. *Quart. J. Roy. Meteor. Soc.,* **114**, 639–964.

Twomey, S., 1974: Pollution and the planetary albedo. *Atmos. Environ.*, **8**, 1251-1256.

Webster, P.J., E.F. Bradley, C.W. Fairall, J.S. Godfrey, P. Hacker, R.A. Houze, R. Lukas, Y. Serra, J.M. Hummon, T.D.M. Lawrence, C.A. Russell, M.N. Ryan, K. Sahami, P. Zuidema, 2002: The JASMINE pilot study. *Bull. Amer. Meteor. Soc,* **83**, 1603-1630.